

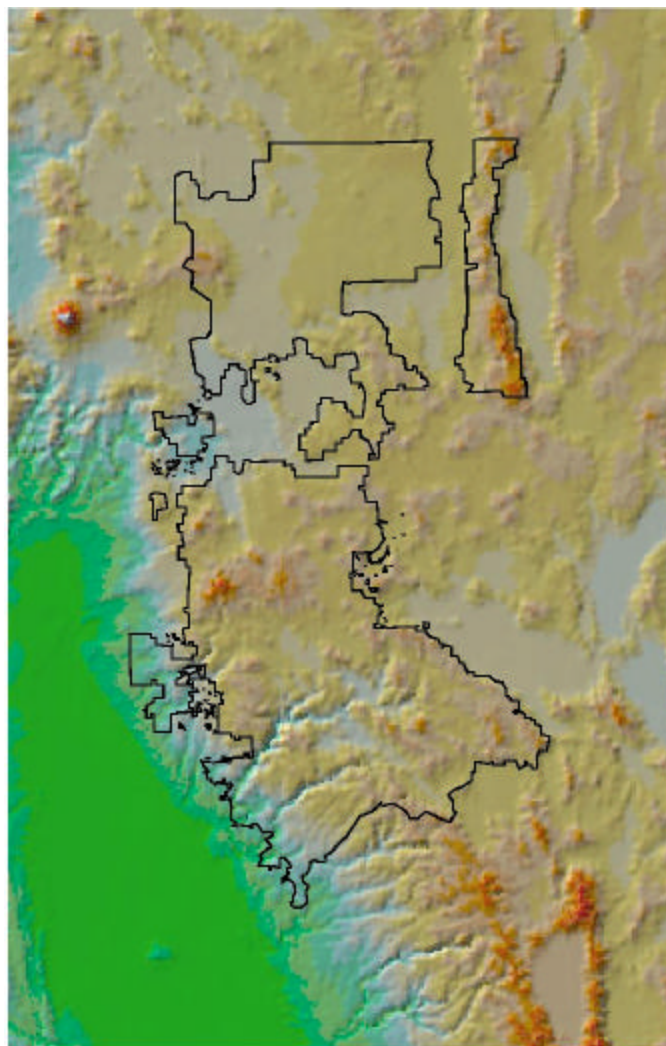
Final Report of the MLP climate and biophysical mapping project

September, 2001

NIKLAUS E. ZIMMERMANN¹ & DAVID W. ROBERTS²

¹Swiss Federal Research Institute WSL, 8903 Birmensdorf, Switzerland;

²Utah State University, Logan, UT 84322-5215, USA



Address of authors:**Niklaus E. Zimmermann**

Swiss Federal Research Institute WSL
Zuercherstr. 111
CH-8903 Birmensdorf
Switzerland

Tel: +41-1-739-2337

Fax: +41-1-739-2215

E-mail: niklaus.zimmermann@wsl.ch

David W. Robertss

Dept. of Forest Resources
Utah State University
Logan, UT 84322-5215
USA

Tel: +1-435-797-2416

Fax: +1-435-797-4040

E-mail: dvrbts@nr.usu.edu

Table of content

1. General objectives and project goals	4
2. Rationale for using DAYMET instead of PRISM	6
3. A brief introduction to DAYMET climate maps	7
4. Methods	7
4.1 The method of downscaling.....	7
4.2 Topographic position	9
4.3 Potential global solar radiation.....	9
4.4 Minimum and maximum temperature	10
4.5 Precipitation	11
4.6 Average temperature.....	11
4.7 Average daytime temperature	11
4.8 Degreeedays.....	12
4.9 Saturated and ambient vapor pressure.....	12
4.10 Vapor pressure deficit.....	13
4.11 Relative air humidity	13
4.12 Potential evapotranspiration (Jensen-Haise & Turc).....	14
4.13 Moisture balance	14
4.14 Moisture index.....	15
4.15 Other available DAYMET 1km grids	15
5. Discussion.....	16
6. References	17

Final Report of the MLP climate and biophysical mapping project

1. General objectives and project goals

The general objectives of the MLP climate and biophysical mapping project were to generate a set of fine-scale (30m) gridded climate maps of the Modoc, Lassen and Plumas National Forests suitable for GIS-based ecological analyses and modeling and for inclusion in Forest Service databases, preferably using Arc/Info. The primary and general approach to fulfil these objectives was to downscale PRISM climate maps from 4.2km to grids of 30m of spatial resolution. The Forest Service provided the PRISM maps, a 30m DEM and additional climate stations data. It was not clear at the beginning of the project, whether the Forest Service would provide soil maps and/or geology maps associated with expert rules to derive soil properties for various geology layers and topographic positions. Site water balance mapping would require the estimate of the water holding capacity of soils.

After DEM and PRISM maps were delivered in February 2001, we concluded to a) use DAYMET instead of PRISM maps for input into the downscaling procedure and b) to drop site water balance modeling, due to the lack of soil properties maps (soil maps or geology maps). DAYMET, newly available since early 2001, offered several advantages for downscaling, which are outlined below in Chapter 2. We agreed to produce the items 1-6, 13, 14 from Table 1, and to provide the original map items 7 & 9 (in 1km spatial resolution) projected to MLP standards (UTM, zone 10). During the generation of the maps, we developed some additional routines to generate other derived climate grids. These were applied to the MLP raster as well, so that they represent an additional benefit. Table 1 lists all data available as 30m grids for the MLP domain.

Table 1: Available climate and biophysical maps in 30m spatial resolution for the MLP domain. The equations referenced are explained in the methods section. The maps are present as ArcInfo grids. In order to keep disk usage as low as possible, all grids were integerized. The z-units of the maps were adjusted accordingly, to maintain reasonable ranges within the grids (e.g. temperature was converted to 1/100°C units). The “basis”-column indicates the degree of derivation. According to this, *etpt* is a highly derived map, compared to *tmin* because it is based on re-calculations of previously derived maps (see chapter 5 for a discussion of the degree of derivation).

	Abbr	Map	Method	Basis	units
1	<i>topo</i>	Topographic Position	ch. 4.2	DEM	[+∞ → -∞]
2	<i>sfmm</i>	Potential global radiation	ch. 4.3	DEM	[kJ/m ² /day]
3	<i>tmax</i>	Maximum temperature	ch. 4.1; 4.4	Daymet, DEM	[1/100 °C]
4	<i>tmin</i>	Minimum temperature	ch. 4.1; 4.4	Daymet, DEM	[1/100 °C]
5	<i>prec</i>	Precipitation	ch. 4.1; 4.5	Daymet, DEM	[1/100 cm]
6	<i>tave</i>	Average temperature	ch. 4.6	3, 4	[1/100 °C]
7	<i>tday</i>	Daytime temperature	ch. 4.7	3, 4	[1/100 °C]
8	<i>ddeg</i>	Degreedays	ch. 4.8	6	[°C * days]
9	<i>vpam</i>	Actual (ambient) vapor pressure	ch. 4.9	4	[Pa]
10	<i>vpsa</i>	Saturated vapor pressure	ch. 4.9	7	[Pa]
11	<i>vpdd</i>	Vapor pressure deficit	ch. 4.10	9, 10	[Pa]
12	<i>relh</i>	Relative humidity	ch. 4.11	9, 10	[per mille; =1/10%]
13	<i>etpj</i>	Pot. Evapotranspiration: Jensen-Haise	ch. 4.12	2, 6	[1/10 mm/day]
14	<i>etpt</i>	Pot. Evapotranspiration: Turc	ch. 4.12	2, 6, 12	[1/10 mm/day]
15	<i>mbal</i>	Moisture Balance	ch. 4.13	5, 14	[ratio]
16	<i>mind</i>	Moisture Index	ch. 4.14	5, 14	[1/100 cm]

Table 1 lists 3 basic climate variables (*tmin*, *tmax*, *prec*), and two basic terrain derived variables (*topo*, *sfmm*). All other variables are deducted from these basic maps, using a set of empirically- or physically based equations. Even though we usually gain ecological significance by using more meaningful parameters (often deducted), we loose – in general – accuracy due to error propagation (specifically with empirical methods, like those to derive potential evapotranspiration). We did not test in detail the accuracy of the maps due to a lack of data. However, when using these climate maps, e.g. for predictive distribution modeling, it is comparably easy to test and mutually compare the predictive power of these biophysical parameters. If the gain in significance compensates the increase of error, then a derived map is more *useful*, even if the error is higher.

Table 2 lists all original DAYMET maps, which were clipped to the MLP domain and re-projected from *Lambert Azimuthal Equal Area* projection to MLP standards (UTM, zone 10; using the BILINEAR re-projection method). These original data are available at 1km of spatial resolution. All climate maps are provided as monthly coverages of 18-year normals (1981-1998) daily data or monthly sums. For some climate variables, the day-to-day variability within the respective months is additionally provided (indicating the degree of local day-to-day variability of this parameter).

Table 2: Available climate and biophysical maps at 1km of spatial resolution for the MLP domain. The equations referenced are explained in the methods section. The maps are present as ArcInfo grids. Since these maps are only available at coarse spatial resolution, no conversion of floating point to integer values was performed. Thus, the z-units deviate from the 30m grids. They are in standard units, used in most applications. The “basis”-column indicates whether this climate map is an original, unaltered grid, or whether it is a simple deduction of available maps.

	Abbr	Map (1km resolution)	Method	Basis/Origin	Units
1	<i>ddeg</i>	Degree-days of growing season	-	Daymet	[°C*day]
2	<i>ddgc</i>	Cooling degree-days	-	Daymet	[°C*day]
3	<i>ddgh</i>	Heating degree-days	-	Daymet	[°C*day]
4	<i>pave</i>	Average precipitation event size	-	Daymet	[cm/rain-day]
5	<i>pfrq</i>	Average number of rainfall events	-	Daymet	[# days/month]
6	<i>prec</i>	Precipitation sum	-	Daymet	[cm]
7	<i>radd</i>	Daily global radiation	-	Daymet	[W/m ²]
8	<i>radv</i>	Day-to-day variability in <i>radd</i>	-	Daymet	[W/m ² /day]
9	<i>tave</i>	Daily average air temperature	-	Daymet	[°C]
10	<i>tavv</i>	Day-to-day variability in <i>tave</i>	-	Daymet	[°C/day]
11	<i>tfro</i>	Number of frost days	-	Daymet	[# days]
12	<i>tmax</i>	Daily maximum air temperature	-	Daymet	[°C]
13	<i>tmin</i>	Daily minimum air temperature	-	Daymet	[°C]
14	<i>tmnv</i>	Day-to-day variability in <i>tmin</i>	-	Daymet	[°C/day]
15	<i>tmxv</i>	Day-to-day variability in <i>tmax</i>	-	Daymet	[°C/day]
16	<i>vpam</i>	Daily average water vapor pressure	-	Daymet	[Pa]
17	<i>vpdv</i>	Day-to-day variability in <i>vpdd</i>	-	Daymet	[Pa/day]
18	<i>tday_n</i>	Daily average day-time temperature	ch. 4.7	12, 13	[°C]
19	<i>vpsa_n</i>	Daily average saturated vp	ch. 4.9	18	[Pa]
20	<i>vpdd_n</i>	Daily average vapor pressure deficit	ch. 4.10	16, 19	[Pa]
21	<i>relh_n</i>	Daily average relative air humidity	ch. 4.11	16, 19	[ratio: 0 - 1]

Only the last four variables (*tday*, *vpsa*, *vpdd*, *relh*) were derived from other, available DAYMET maps. They are (on the CD) characterized with the extension “_n” to show clearly, that they are not of DAYMET origin directly. It is important to understand that all of the original DAYMET maps (except the basic *tmin*, *tmax*, *prec*), were all derived from these three basic maps. However, other than in our downscaling exercise, the deductions were calculated on a daily basis. Thus, we expect differences

between 30m and 1km maps, specifically where new 1km maps were derived on a daily basis (and then summarized into monthly values), while the new 30m maps were derived from monthly summaries directly.

2. Rationale for using DAYMET instead of PRISM maps

A preliminary study has proven that DAYMET and PRISM maps are of equal quality (Stillman et al., 1996), thus from an accuracy point of view, they are both well-suited as a basis for downscaling. However, DAYMET offers considerable advantages over PRISM, from a more theoretical point of view for downscaling, especially for temperature. The advantage of DAYMET originates from the method temperature maps are generated. In the PRISM approach, all input (climate) stations elevations are altered to a mean elevation of the coarse-scale DEM at the stations location. Using a 4.2km DEM causes significant changes in the stations elevations. These altered elevations go into the regression where the elevational lapse rates and the intercept are determined through local regressions of all stations of the same facet (terrain element). This approach has shown to be highly suited for precipitation (Daly et al., 1994). For temperature, this approach does not yield optimal results. Using the “true” station elevations has provided better results for a large area in the northwest of the USA (Thornton et al., 1997). The reason for this is that precipitation responds much more regionally to general mass uplifts, independent of small scale terrain features. Temperature, on the other hand, responds much more predictably as a function of elevation or latitude. Obviously, the resulting coarse-scale maps are of similar quality. However, when it comes to downscaling, the PRISM approach (applied to both precipitation and temperature) is less suited for using a mowing window regression technique. When mowing window regressions are calculated between coarse DEM pixels and coarse climate grids, then we can theoretically only downscale to finer grids, when the original regressions are based on “accurate” stations elevations. Otherwise, the original regression values used to generate the original climate maps are conceptually hard-bound to the coarse DEM, and do not allow the downscaling to finer-scale DEMs¹. DAYMET does not alter stations elevations for temperature-elevation regression.

In addition, PRISM uses a “facet” approach, where climate stations of the same terrain facet (general large-scale slope element) only are used in regional regressions. This method is highly suited to detect and map sharp climate gradients as established across the coastal range from west to east. This method is, however, sensitive to classifying the terrain properly. Once a pixel is classified as “rain shadow” e.g., it will receive considerably less rain than neighboring pixels, if the latter are classified differently. One such problem within the MLP domain was reported to the PRISM team (S. Smith, pers. comm.), and it turned out to be such a terrain classification problem. A comparison with original (1km) precipitation values of DAYMET showed, that the latter model was unaffected by this problem. No such error was found.

And finally, even for precipitation, the facet approach is conceptually less suited for downscaling of precipitation, because pixels of a mowing window do not necessarily belong to the same facet, and thus it is not possible to detect the “hidden” regression parameters properly. However, the latter is not a serious problem, since the regression still yields useful results, if the climate is mapped accurately.

In conclusion, we decided to use DAYMET data to downscale temperature maps from 1km to 30m pixel size. Precipitation was also downscaled using DAYMET origin. However, the maps were only downscaled

¹ Originally, regional regressions were performed to establish the general dependence of a climate parameter on elevation, when DAYMET or PRISM maps were developed. These regression values were then applied to the coarse DEM to generate climate maps. It is important to understand that applying a mowing window regression aims at detecting the regression parameters originally used to generate the climate maps. Once these regression values are re-covered, we can interpolate and apply them to smaller scale DEMs of our choice.

to a resolution of 250m. This is considered as the finest resolution precipitation maps should be generated for, because below this spatial scale precipitation behaves unpredictable anyway (P.E. Thornton, pers. comm.). In order to provide a common spatial resolution for the MLP mapping, we then further re-sampled the 250m precipitation maps by linearly interpolating to 30m. This is conceptually the best way to read precipitation at this resolution, since we do not at non-significant terrain variation to precipitation.

3. A brief introduction to DAYMET climate maps

The development of the DAYMET routine goes back to the MT-CLIM model (Running et al., 1987; Hungerford et al., 1989), which was used to adjust and extend the data of a low elevation climate station to a target locations upslopes at any other elevation. This model was used extensively for generating input data for ecosystem process models like FOREST-BGC (Running & Gower, 1991, Running, 1994). Later, BIOME-BGC was developed and even extended significantly compared to the FOREST-BGC origin (Thornton, 1998). BIOME-BGC is developed as both a single point and a gridded model version. The single point version was developed at the NTSG lab of the University of Montana in Missoula, MT and is available at (<http://www.forestry.umt.edu/ntsg/Bioclimatology/>). The gridded model version requires an extensive set of daily climate input data, available at the spatial scale of the model grids. For this purpose, DAYMET was developed (Thornton et al., 1997; Thornton, 1998; Thornton & Running, 1999; Thornton et al., 2000). This model generates daily climate grids using simple climate stations input data.

Recently, the DAYMET model was applied to the whole territory of the US using a 1km DEM and a set of approx. 8000 climate stations for the period of 1981-1998. The maps were developed in 2000-2001 at the NTSG lab, University of Montana, MT, USA, for input into large-scale ecosystem process modeling. The DAYMET model generates a set of 5 thematic maps at daily temporal resolution, namely minimum and maximum temperature, precipitation, global radiation, and vapor pressure (deficit). The resulting daily climate maps were then further summarized into 18 years monthly normals and to various derived parameter maps (as e.g. monthly average number of precipitation days, average monthly amount of rainfall per rain day, etc.). The monthly data are soon available for free download from the internet (www.daymet.org), or for a reasonably low processing fee, if ordered as a set of 34 CDs.

A preliminary study in the Central Rocky Mountains has shown that DAYMET and PRISM maps are of equal quality for mapping precipitation, and both are somewhat more precise compared to the Spline-based ANUSPLIN model of Hutchinson (Stillman et al., 1996).

4. Methods

Details of the methods used to generate new or downscaled maps, as well as derived biophysical modeling products are described below. The description does not go into details with regards to the DAYMET model. It only explains DAYMET procedures where it is necessary to understand the downscaling method. For DAYMET methodologies, we refer to the original publication (Thornton et al., 1997).

4.1 The method of downscaling

To generate fine-scale climate maps, we downscale coarse-gridded climate maps (e.g. DAYMET or PRISM) based on a moving window regression technique. To do this, a window is defined (width, height), and the window is moved over the whole study area, row-by-row and column-by-column (Fig. 1). This is done simultaneously over two grids, 1) a DEM and 2) a climate grid of interest (e.g. *t_{max}* of July). At every window position, all grid cells within the window are sampled pairwise (elevation and *t_{max}*).

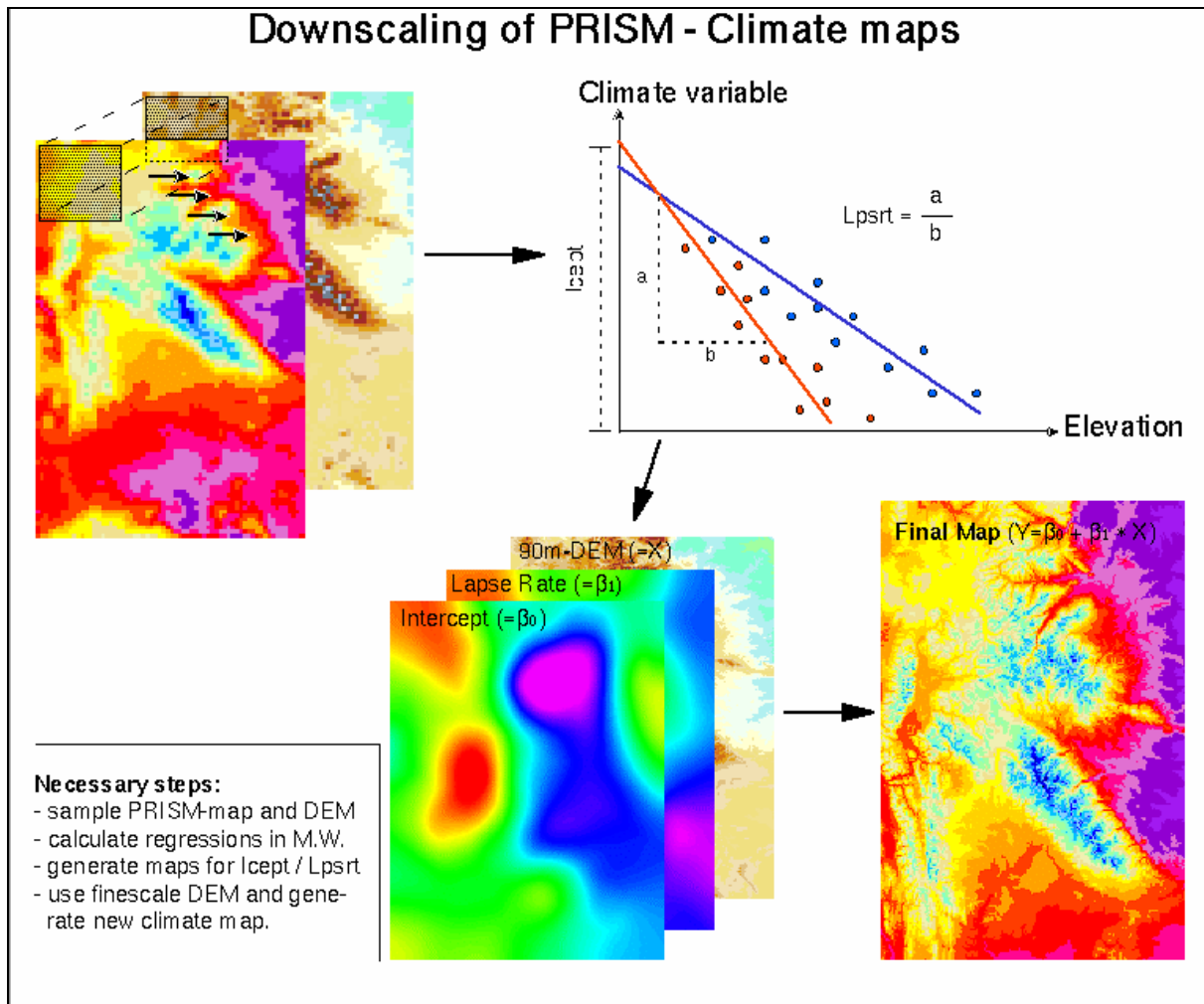


Figure 1: Illustration of the downscaling procedure using an example of PRISM climate maps for North-western Wyoming (Yellowstone area, Shoshone National Forest, Windriver Range).

Subsequently, a linear regression is applied to these pairs of elevation and climate data at one window position, resulting in a lapse rate and an intercept per window position. These results are saved to the center cell of each window position. Once the moving window regression is terminated, we now have two new, coarse-scale grids containing the moving window regression parameters. The new grid is slightly smaller than the original grid ($-0.5 \cdot \text{window size}$ at each border) due to the fact that the results of the moving window regression are saved to the center cell.

The new regression grids are now spatially interpolated to a finer spatial scale, namely to the scale of a fine-scale DEM, which represents the basis for the new, fine-scale climate grids. Finally, the regression grids are re-projected to actual, fine-scale elevation values using the detailed DEM and by applying the regression parameters (local lapse rate and intercept, see figure 1). The method described here is also illustrated under <http://www.wsl.ch/staff/niklaus.zimmermann/biophys.html#Meth> (see Fig. 2, there).

4.2 Topographic position

[Range: - $\frac{3}{4}$ + $\frac{3}{4}$]

Topographic position is a useful measure to express the exposure of a location in space compared to the surrounding terrain. Positive values express relative ridges, tops, exposed sites, and the measure summarizes various micro- to meso-climatic and edaphic features, such as comparably high winds and droughts, shallow soils, low nutrient status, etc. Negative values, on the other hand, stand for sinks, gullies, valleys or toe slopes, and the measure summarizes various micro- to meso-climatic and edaphic features, such as comparably good wind shelter, water and nutrient status, deep soils.

The method used allows to identify topographic exposure (ridge, slope, toe slope, etc) at various spatial scales, and to hierarchically integrate these features into a single grid. Circular moving-windows with increasing radii are applied to a DEM, and the difference between the average elevation of the window and the center cell of the window is calculated and written to exposure grids. The resulting maps are interpreted as *relative topographic exposure* at a given spatial scale (the search radius). The exposure can be interpreted as a ridge or peak if the center cell in the moving window has a higher elevation than the average elevation of the cells in the window. Contrarily if the center cell is of lower elevation than the average elevation of the window, then the center pixel can be interpreted as "toe slope" or "valley bottom" (depending on the difference). A hierarchical integration into a single map is achieved by starting with the standardized exposure values of the largest window, then adding standardized values from smaller windows where the (absolute) values of the smaller (search-) scale grids exceed the values of the larger scale map. Finally, the integrated map is smoothed using a 3x3 cell moving window.

The resulting map of topographic position now incorporates exposure at various spatial scales. It basically keeps the most extreme exposure integrated over all scales used. In the MLP project, we used a window of circular moving window of 120m as the smallest search area. Subsequent larger hierarchies included 720m, 1320m, up to 6120m (at steps of 600m). A more detailed description of the AML we developed is available at http://www.wsl.ch/staff/niklaus.zimmermann/programs/aml4_1.html.

Note: Usually, plants respond to topographic extremes at various spatial scale. Both small and large ridges result in comparably dry soils and high winds. However, animals usually do not react to the same range of spatial scales. Therefore, it would be more appropriate to use the topographic exposure maps that best correspond to the respective animal species studied.

Available: All individual exposure maps are available at 30m of spatial resolution (*exp2nrm*, *exp12nrm*, ... *exp102nrm*), and the integrated topographic position maps are available in an un-smoothed (*topo_30m*) and in a smoothed version (*topos_30m*). The "2" in *exp2nrm* represents the number of pixels of the search window radius. Thus, the *exp2nrm* grid represents the individual, normalized exposure grid of the 120m (diameter) circular search window.

4.3 Potential global solar radiation

[Unit: kJ /m²/day]

Several methods to calculate potential direct and diffuse solar radiation over large spatial scales have been developed recently in a GIS environment (Dubayah and Rich, 1995; Rich et al., 1995; Kumar et al., 1997). However, these methods are only available in a general form for clear-sky radiation. More information on atmospheric transmittance is necessary to include the radiation reduction due to atmospheric conditions. So, most programs ask for a general transmittance term, or they just calculate potential instead of actual global radiation. We used a method developed by Kumar et al. (1997) to calculate such potential solar radiation maps (direct and indirect), over the 30m MLP DEM. This method incorporates shadowing by neighboring terrain. The program was tested and corrected for errors that gave wrong results at northern hemispheres.

To generate 30m grids of potential global radiation, we developed solar radiation maps (a: direct and b: diffuse) of each 10th Julian day. These maps were added up to daily potential global radiation values (diffuse + direct). We then used 4-point (*Simpson's rule*) and 5-point (*Bode's rule*) interpolation

techniques to integrate the calculated daily radiation maps into monthly averages of daily data ($\text{kJ/m}^2/\text{day}$). For an overview of the methods to calculate direct and diffuse solar radiation, as well as a list of available AMLs, see: <http://www.wsl.ch/staff/niklaus.zimmermann/programs/aml.html>.

Another pathway to generate solar radiation grids was developed by Thornton et al. (1997) in DAYMET radiation values. Their method does not include shadowing by neighboring terrain. However, they use a modified Bristow & Campbell (1984) method to calculate the daily atmospheric transmittance based on the diurnal temperature range (Thornton & Running, 1999; Thornton et al., 2000). This method has been shown to successfully predict a large proportion of the variation in daily radiation fluxes (Running et al., 1987; Glassy & Running, 1994). Since it is based directly on daily minimum and maximum temperatures, this method cannot be downscaled as monthly averages. Thus, the resulting radiation values are not potential, but actual global radiation values (in W/m^2 units).

We prepared the original 1km global radiation maps (18-year monthly averages), as well as the 18-year monthly day-to-day variation in global radiation. The latter is a measure of expected variability of daily values around the mean, provided in the monthly average maps.

Note: Global radiation is generally said to be a direct site factor, having a direct influence on plant physiology. Therefore, it is an important factor to explain plant distribution and abundance. The potential global radiation does not include regional reduction of the atmosphere due to variable atmospheric transmittance (moisture, cloudiness, etc.). It only includes changes in the atmospheric mass due to variable length of the solar path through the atmosphere. Thus it is not capturing the “true” energy balance, rather it is capturing the relative differences between pixels. Compared to the DAYMET routine, however, this method includes shadowing due to high adjacent terrain. No method has been implemented so far, which easily combines the two approaches.

Available: All individual monthly maps of potential global solar radiation are available at 30m of spatial resolution (*sfmm01_30m*, *sfmm02_30m*, etc.), and the actual global radiation grids are available as 1km grids (*radd01*, *radd02*, etc.).

4.4 Minimum and maximum temperature

[Unit: °C, °C/100]

The basic climate parameters *tmin* and *tmax* are available at both the 30m and the 1km resolution. They are both generated at 30m grid size using the moving window regression technique. For temperature, we chose a window size of 25x25 pixels (=625 total). In order to cope with missing values, a minimum threshold of 160 pixels was set, required to perform the local regressions. The original DAYMET climate and DEM grids (in *Lambert Azimuthal Equal Area* projection) were sampled as a point lattice (using the *gridspot* command) and then re-projected to UTM, zone 10 as a point file, in order to avoid distortions of grid cells.

To generate reasonably sized grids, we converted all temperature grids to 1/100 °C units. This allows to shrink the size of the grids up to 85%, while maintaining the basic variability. This is not necessary for the 1km DAYMET grids.

Note: Compared to precipitation, the downscaling of temperature grids is best done with larger moving windows. This reflects the fact that lapse rates and intercepts of temperature vary less within short distances. Thus we gain accuracy by including potentially more terrain. On the other hand, if we choose to large areas, the regression becomes again inaccurate, because we have too much of regional variation within the window.

Available: All individual monthly maps of average daily minimum and maximum temperature are available at both 30m (*tmin01_30m*, *tmax01_30m*, etc.), and 1km of spatial resolution (*tmin01*, *tmax01*, etc.).

4.5 Precipitation

[Unit: cm, cm/100]

The 18-year average monthly precipitation sum is the third of the basic climate parameters (besides *tmin* and *tmax*), used to derive a set of new maps thereof. The precipitation grids are downscaled from 1km DAYMET origin to 30m of spatial resolution with the same basic moving window downscaling technique that was applied to *tmin* and *tmax*. Contrary to temperatures, we chose a smaller moving window, i.e. 15x15 pixels of size. This amounts to 225 cells per window position. Again the minimum threshold required to calculate a local regression was set to 160 pixels per window. Besides, the procedure to downscale precipitation grids was equal to generating temperature maps.

To generate reasonably sized grids, we converted all monthly precipitation maps to 1/10mm units (=mm/10). This allows to shrink the size of the grids as much as 85%, while maintaining the basic variability also in months with low precipitation sums. This is not necessary for the 1km DAYMET grids, where the basic unit is cm.

Note: Compared to temperature, the downscaling of precipitation grids is best done with smaller moving windows. This is because lapse rates are less clearly linked to general topography and vary more across a landscape. Rather, local intercepts are important (to be calibrated). This reflects the fact that precipitation follows general masses (of mountain ranges) independent of small topographic variations (in elevation). With too small windows, there are not enough pixels to perform an accurate regression estimate. Again, this is comparably unimportant (compared to temperature), since the regression intercepts is more important, when lapse rates are close to zero.

Available: All individual monthly maps of precipitation sum are available at both 30m (*prec01_30m*, *prec02_30m*, etc.), and 1km of spatial resolution (*prec01*, *prec02*, etc.).

4.6 Average temperature

[Unit: °C, °C/100]

The daily average temperature is derived simply by averaging *tmin* and *tmax*. If only daily data is available, this is a meteorological standard (eqn. 1):

$$T_{ave} = \frac{(T_{min} + T_{max})}{2} \quad (1)$$

To generate reasonably sized grids, we converted all temperature grids to 1/100 °C units. This allows to shrink the size of the grids up to 85%, while maintaining the basic variability. This is not necessary for the 1km DAYMET grids.

Available: All individual monthly maps of average daily temperature are available at both 30m (*tave01_30m*, *tave02_30m*, etc.), and 1km of spatial resolution (*tave01*, *tave02*, etc.).

4.7 Average daytime temperature

[Unit: °C, °C/100]

The daily average daytime temperature is derived from *tmin* and *tmax* using the method of MT-CLIM and DAYMET (eqn. 2). This is an important map to calculate the saturated (daytime) vapor pressure, necessary to calculate the average daily vapor pressure deficit or the relative humidity of a specific month.

$$T_{day} = (0.394 \cdot T_{min} + 0.606 \cdot T_{max}) \quad (2)$$

DAYMET maps are not available for daytime temperature. Thus we generated the average monthly daytime temperature using eqn. 2. To generate reasonably sized grids, we converted all temperature grids to 1/100 °C units. This allows to shrink the size of the grids up to 85%, while maintaining the basic variability. This is not necessary for the 1km DAYMET grids.

Available: All individual monthly maps of average daytime temperature are available at both 30m (*tday01_30m*, *tday02_30m*, etc.), and 1km of spatial resolution (*tday01*, *tday02*, etc.).

4.8 Degreedays

[Unit: °C*days]

The concept of degreedays is often used in environmental modeling (e.g. it represents a basic driver of models of the JABOWA-FORET gap model family, Shugart, 1984). Here, the daily amount of energy (°C) above a threshold is summed up over a period of days (eqn. 3).

$$DDEG = \sum_{j=1}^n \max[0, (T_j - T_0)] \quad (3)$$

where T_j = daily average temperature, T_0 = threshold value, and n = the number of subsequent days. The values are summed up over the period of n days where $T_j > T_0$ (Tuhkanen 1980). The threshold value T_0 is considered the minimum temperature for plant growth. In this study, we used a threshold of 0.0°C. The original DAYMET 1km degreeday grids are summed over daily values for each months, while for the downscaled 30m grids, we interpolated a single yearly degreeday map based on monthly average temperature values using trapezoid interpolations between months. Both, the 1km monthly grids and the 30m yearly degreeday sum are in units of °C*days.

Note: A range of values of the threshold T_0 is applied in different studies. For global perspectives, this threshold is often set to 5.56°C (=18°F), as e.g. in Prentice et al. (1992), while other applications, specifically for high elevation and Boreal/Arctic studies, employ a threshold value of 0.0°C (Thornton et al., 1997). As long as we do not imply a physiological mechanism with this value (e.g. chilling risk), we are not constrained to a specific threshold. Rather, we use differences in degreedays as variations in basic heat sum (or energy) requirements of plants to grow.

Available: All individual monthly maps of average daytime temperature are available at 1km of spatial resolution (*ddeg01*, *ddeg02*, etc.), and the yearly degreeday map at 30m of spatial resolution (*ddeg*).

4.9 Saturated and ambient vapor pressure

[Unit: Pa]

Vapor pressure is a function of amount of humidity per volume unit air mass and the air temperature. At dew point temperature, the humidity is 100%, and the related vapor pressure can be calculated by eqn. 4. Considering that the night-time minimum temperature is a reasonable surrogate for dew point temperature then the ambient vapor pressure vp_{amb} can be calculated by replacing T_{dew} by T_{min} in eqn. 4. This assumption has proven to be sufficiently accurate (Running et al., 1987; Glassy and Running, 1994) but to a lesser degree in very dry environments (Kimball et al., 1997).

$$VP_{amb} = 610.78 \exp \left[\frac{17.269 \times T_{dew}}{237.3 + T_{dew}} \right] \quad (4)$$

where T_{min} is used instead of T_{dew} for our calculations. In order to assess the relative humidity or the vapor pressure *deficit*, we need to calculate the potential vapor pressure of saturated air for daytime temperature. Therefore, we apply eqn. 5 equal to eqn. 4 where T_{dew} is replaced with T_{day} (eqn. 2):

$$VP_{sat} = 610.78 \exp \left[\frac{17.269 \times T_{day}}{237.3 + T_{day}} \right] \quad (5)$$

To generate reasonably sized grids, we converted all vapor pressure grids to integer values. This allows to shrink the size of the grids up to 85%, while maintaining the basic variability. This is not necessary for the

1km DAYMET grids. The basic unit of vapor pressure grids is Pa. DAYMET provided ambient, but not saturated vapor pressure maps. The latter were thus generated based on eqn. 5 and monthly daytime temperature maps.

Note: The DAYMET maps of average monthly ambient vapor pressure is calculated from daily minimum temperature data. Averaging these daily values to monthly maps is not equal to calculating average monthly minimum temperatures and then calculate average monthly ambient vapor pressures from monthly minimum temperature. Therefore, we get deviations in the ambient vapor pressure maps as generated by DAYMET approaches compared to our method based on downscaled 30m T_{min} maps.

Available: All individual monthly maps of ambient and saturated (average daily) vapor pressures are available at both 30m ($vpam01_30m$, $vpas01_30m$, etc.), and 1km of spatial resolution ($vpam01$, $vpas01$, etc.).

4.10 Vapor pressure deficit

[Unit: Pa]

Average monthly vapor pressure deficit is the difference in vapor pressure between saturated and ambient air humidities (eqn. 6)

$$VP_{deficit} = VP_{sat} - VP_{amb} \quad (6)$$

where: VP_{sat} = saturated vapor pressure (eqn. 4) and VP_{amb} = ambient vapor pressure fields (eqn. 5). To generate reasonably sized grids, we converted all 30m vapor pressure deficit grids to integer values. This allows to shrink the size of the grids up to 85%, while maintaining the basic variability. This is not necessary for the 1km DAYMET grids. The basic unit of vapor pressure deficit grids is Pa. The 1km vapor pressure deficit grids were not available from DAYMET origin, thus we generated this map based on eqn. 6 and using VP_{sat} and VP_{amb} .

Note: Vapor pressure deficit is an important control of stomatal conductance. This value is thus often used in physiology based photosynthesis models. Due to its importance for plant photosynthesis and stomatal conductance controls, it is a key parameter to understand and predict the distribution, growth and performance of plants in space.

Available: All individual monthly maps of (average daily) vapor pressure deficits are available at both 30m ($vpdd01_30m$, $vpdd02_30m$, etc.), and 1km of spatial resolution ($vpdd01$, $vpdd02$, etc.).

4.11 Relative air humidity

[Unit: ratio, %/10]

A similarly important (and closely correlated) value is the relative air humidity. Again, average daily values of relative air humidity is a key control of stomatal conductance.. By this, it controls the flow of water from soils to the atmosphere, and it has a limiting control of photosynthetic activity of leafs. Relative air humidity is calculated using eqn. 7:

$$relH = \frac{VP_{amb}}{VP_{sat}} \cdot 100\% \quad (7)$$

All 30m maps are integerized in order to limit the disc space requirements of the monthly averages of relative humidity. The basic unit of this parameter is per cent (%). The 1km grids are not converted to integer values. Here, the unit is just the ratio (without multiplication to %).

Note: Due to differences in the calculations of ambient vapor pressure (see notes under 4.9), the relative humidity values of the 30m maps differ from those of the 1km version.

Available: All individual monthly maps of (average daily) relative air humidity are available at both 30m ($relh01_30m$, $relh02_30m$, etc.), and 1km of spatial resolution ($relh01$, $relh02$, etc.).

4.12 Potential Evapotranspiration (Jensen-Haise & Turc)

[Unit: cm, cm/100]

A range of empirical methods have been developed to calculate potential evapotranspiration. While the physically-based, modified Penman-Montheit equation requires a set of unavailable variables, several empirical methods are available that allow to calculate ETP for the MLP domain. We chose two methods that are well suited and comparably accurate according to Schrödter (1985) and Müller (1989). Compared to simpler empirical methods, they are both based on multiple variables to explain potential evapotranspiration.

Jensen-Haise method

The Jensen-Haise empirical equation is based on monthly average daily global solar radiation and temperature. It has been developed specifically for the arid area of the Intermountain West (Jensen & Haise, 1963). The Jensen-Haise potential evapotranspiration is calculated as follows:

$$ETP_{jen} = \left[0.245 \times 10^{-4} \times R_s \times ((0.025 \times T_{ave}) + 0.08) \right] \quad (8)$$

where: T_{ave} is the average daily temperature (t_{ave}) in °C, and R_s is the global radiation in kJ/m²/day. We used the potential global radiation for calculating $etpj$.

All 30m maps are integerized in order to limit the disc space requirements of the monthly averages of potential evapotranspiration. The basic unit of this parameter is 1/100 cm (0 1/10 mm).

Turc method

The Turc empirical equation is based on monthly averages of daily global solar radiation, temperature, and relative air humidity. The method has been developed and extensively used in France, and it is specifically suited for areas with strong gradients in air humidity. The Turc method includes relative humidity as a corrective factor as soon as the monthly average relative humidity is below 50% (Turc, 1963). The Turc potential evapotranspiration is calculated as follows:

$$ETP_{trc} = \left[((0.0239 \times R_s) + 50.0) \times \left(\frac{T_{ave}}{T_{ave} + 15.0} \right) \times \max \left(1.0, \left(1.0 + \frac{50 - relH}{70} \right) \right) \times \left(\frac{0.4}{30.0} \right) \right] \quad (9)$$

where: T_{ave} is the average daily temperature (t_{ave}) in °C, R_s is the global radiation in kJ/m²/day, and $relH$ is the relative air humidity in %. We used the potential global radiation for calculating $etpt$.

All 30m maps are integerized in order to limit the disc space requirements of the monthly averages of potential evapotranspiration. The basic unit of this parameter is 1/100 cm (0 1/10 mm).

Note: Due to the fact that DAYMET calculated radiation in Watt/m² it is not easily possible to convert this value to kJ/m²/day, since we do not know exactly the day-length used in the DAYMET calculations. Thus we did not calculate the 1km version based on DAYMET maps.

Available: All monthly maps of (average daily) potential evapotranspiration are available at a spatial resolution of 30m for the Jensen-Haise method ($etpj01_30m$, $etpj02_30m$, etc.) and for the Turc method ($etpt01_30m$, $etpt02_30m$, etc.).

4.13 Moisture balance

[Ratio]

The moisture ratio is often calculated to express the atmospheric humidity balance over a landscape, independent of soil or vegetation properties. It can be interpreted as the potential water balance over this landscape, which then is modified by soil and vegetation attributes. There are several variants available to calculate the moisture balance. The basic similarity is that they are all starting from a ratio between potential evapotranspiration and precipitation. If this ratio is above 1.0, then precipitation exceeds the

potential evapotranspiration (for this month). Values below 1.0 indicate drought, where potentially more water evaporates than is provided by rainfall.

To calculate the moisture balance, we used the Turc-based Etp values, since we have a strong humidity gradient across the MLP bounds. We subtracted a value of 1 from this basic *mbal* ratio, so that we have positive ($prec > etpj$) and negative ($prec < etpj$) values. The values are then multiplied by 1000.0 and integerized, yielding values in per mille (1/10 %).

$$MBal = \text{int} \left(\left(\frac{ETP_{trc}}{P} - 1.0 \right) \times 1000.0 \right) \quad (10)$$

where: P is the average daily precipitation in mm and ETP_{trc} is the average daily potential evapotranspiration in mm. We used the potential global radiation for calculating *etpt*.

Note: Attention, this basic ratio calculation for *mbal* does not provide a mathematical solution for cases where *etpt* is zero. This causes the calculations to be NODATA in the ArcInfo grids for such constellations. This is not the same as a value of zero! The latter indicates a balance of *prec* and *etpt*.

Available: All monthly maps of moisture balance are available at a spatial resolution of 30m (*mbal01_30m*, *mbal02_30m*, etc.). They are calculated using the Turc method for potential evapotranspiration.

4.14 Moisture Index

[Unit: cm/100]

The moisture index is another, often used method to express the atmospheric humidity balance over a landscape. It can be interpreted (equally) as the potential water balance over this landscape, independent of soil and vegetation attributes. This index is not based on a ratio, but rather on the difference in *etpt* and *prec*. The interpretation of the index is similar to the *mbal* ratios. If the index is positive, then precipitation exceeds the potential evapotranspiration (for this month). Values below zero indicate drought, where potentially more water evaporates than is provided by rainfall.

$$MInd = P - ETP_{trc} \quad (11)$$

where: P is the average daily precipitation in mm and ETP_{trc} is the average daily potential evapotranspiration in mm using the Turc method (eqn. 9).

All 30m maps are integerized in order to limit the disc space requirements of the monthly averages of the moisture index. The basic unit of this parameter is 1/100 cm (0 1/10 mm) per month.

Note: Attention, compared to *mbal* the calculation for *mind* does provide a mathematical solution for cases where *etpt* is zero. This does not cause NODATA values in the ArcInfo grids. Compare the note for *mbal* for further information.

Available: All monthly maps of moisture balance are available at a spatial resolution of 30m (*mbal01_30m*, *mbal02_30m*, etc.). They are calculated using the Turc method for potential evapotranspiration.

4.15 Other available DAYMET 1km grids

[Unit: see text for details]

A series of additional DAYMET climate maps are available only at the 1km spatial scale. This is mostly due to the fact that these parameters are not easy to downscale at monthly average values. This is especially true for all day-to-day variability maps. The climate variables are discussed below.

ddgc: Cooling degreedays are a derivative of the concept of degreedays. Here, the threshold T_0 is set to the value of 18°C. The heat sum above 18°C is interpreted as the energy level a house needs to be cooled down for comfortable living. Units are °C*days.

ddgh: *Heating degreedays* are the contrary concept of cooling degreedays. Here, for all days where the average daily temperature is below 18°C, the negative differences to the threshold are summed up, representing the amount of energy necessary to heat up a house for comfortable living.

pave: The monthly *average precipitation event size* characterized the average amount of precipitation (in cm) per rain day. This is equal to dividing the average monthly precipitation sum (*prec*) by the average monthly number of rain days (*pfrq*).

pfrq: The monthly *average number of rainfall events* is the number of rain days per month. This value is helpful to distinguish areas of high precipitation sums with comparably low rainfall frequencies (Mediterranean type climate), from other areas of comparably high precipitation sums paired with high rain frequencies (oceanic type climate).

rdvv: *Day-to-day variability* in global radiation (*radd*) expresses the degree of stability of this parameter. Areas of high variability require specific adaptations (tolerances) by plants and animals.

tavv: *Day-to-day variability in tave* is a measure to distinguish oceanic from continental type climates.

tmxv & tmnv: *Day-to-day variability* in both *tmin* and *tmax*, express similar characteristics as *tavv*.

tfro: The average monthly *number of frost events* is equal to the number of frost days. This is an important characteristics to explain the distribution and performance of frost-sensitive plants and animals.

5. Discussion

A series of downscaled and derived climatic and biophysical maps have been developed for the MLP bounds. This has been achieved by downscaling basic DAYMET maps, and by applying a set of equations to derive physiologically and ecologically more meaningful grids. In order to understand the potential and limitations of the new 30m maps, we discuss below a few important points.

We did not test the individual maps against climate stations data, since the data provided did not cover the time period the DAYMET (and the PRISM) maps were calculated for. Comparing climate maps against climatological summaries of a differing time period does not make sense. However, we checked carefully the plausibility of the calculated values and their summary statistics against the original DAYMET maps. This helps to identify uncertainties and calculation errors.

In some cases, there are differences between derived 30m maps and original 1km DAYMET maps. This is most likely due to the fact that the DAYMET 1km monthly summaries were derived differently from the downscaled 30m maps. The difference is as follows. DAYMET is based entirely on daily climate maps. These basic daily climate maps were then further processed to obtain new derived *daily* maps. Monthly summaries were then calculated based on the derived daily maps. This procedure is not equal to calculating derived maps directly from monthly summaries of basic climate maps. However due to disk space limitations, this is the only possible solution for such small-scale grids. Daily 30m grids for the 18-year period of 1981-1999 for one basic climate parameter would have required 2.438 Terrabytes of disk space (=2438 GB)!

Users of the downscaled and derived 30m have to consider the following restrictions, potential errors and limitations of the climate and biophysical maps:

- The basic accuracy of the climate maps is given by the accuracy of the DEM used to scale climate to the landscape. The MLP 30m DEM has some limitations. It seems that the mosaicking of individual 30m tiles to the whole-area MLP DEM caused some problems. Along the edges of the original tiles, there are channel structures visible (see e.g. the monthly values of global radiation, especially visible in

winter months). Also, some areas have strip features across the DEM. This is not easy to avoid, since we are limited by the quality of the raw data we obtain. These channels have an elevational drop of approx. 10-20 meters. This is not a serious problem for the calculation of most basic and derived climate parameters. However, it becomes visible as soon as radiation based methods are in use. Here, a sharp drop in elevation causes strange terrain features (steep slopes and sharp changes in aspect). Comparably, temperature and precipitation estimates are hardly affected by an error of 20m of elevation.

- With every step of derivation, we propagate the errors of the biophysical maps used to generate the new grids. This means that conceptually, these highly derived maps have higher errors than the more basic climate maps. On the other hand, we gain ecological and physiological significance. E.g. moisture index, soil moisture, or degree-days are more relevant to plants than average yearly temperature and precipitation sums, or even elevation. Thus we have gain in ecological significance with derived maps, and we sacrifice spatial and thematic accuracy. The example of temperature vs. elevation helps to illustrate this problem, also in the context of spatial scales. At one mountain slope, we might be able to predict the upper limit of growth of a plant species easily and accurately by elevation. Over large spatial scale, especially along a north-south gradient, the upper limit of this same plant species will most likely change considerably, and we do not have a simple explanation in terms of a threshold. However, summer temperature might well help us to establish a threshold, because temperature is more likely a mechanistic cause for this growth limit. In GIS-based modeling exercises, we would use DEMs and temperature maps to establish such statistical relationships with plant occurrences. If we only study one mountain slope, we would likely find that elevation has a higher statistical significance to explain the elevational distribution of a plant species, because the spatial uncertainty of elevation maps are lower than those of the derived temperature maps. However, over large areas, temperature is the more significant factor to explain plant distribution, than elevation, since the elevation-temperature relationship changes significantly over this spatial domain. At this scale, we are likely to find a higher statistical significance with temperature, despite the errors accumulated in temperature maps (error of the DEM plus error of the model to derive temperature from climate stations and a DEM). Thus derived maps are not necessarily useless. They help understand ecological processes specifically at large spatial scales despite the problem of error propagation. See Guisan & Zimmermann (2000) for an overview of conceptual and statistical approaches to deal with species-environment relationships, and habitat distribution modeling in ecology and Zimmermann & Kienast (1999) for an example.

6. References

- Bristow, K.L. and Campbell, G.S. 1984. On the relationship between incoming solar radiation and daily maximum and minimum temperature. *Agricultural and Forest Meteorology* **31**: 159-166.
- Daly, C., Neilson, R.P. and Phillips, D.L. 1994. A Statistical-Topographic Model for Mapping Climatological Precipitation over Mountainous Terrain. *Journal of Applied Meteorology* **33**: 140-158.
- Dubayah, R. and Rich, P.M., 1995. Topographic solar radiation models for GIS. *International Journal for Geographical Information Systems*, **9**(4): 405-419.
- Glassy, J.M. and Running, S.W. 1994. Validating diurnal climatology logic of the MT-CLIM model across a climatic gradient in Oregon. *Ecological Applications* **4**: 248-257.
- Guisan, A. & Zimmermann, N.E., 2000. Predictive habitat distribution models in ecology. *Ecological Modelling* **135**(2-3):147-186.
- Hungerford, R.D., Nemani, R.R., Running, S.W. and Coughlan, J.C. 1989. *MT-CLIM: A mountain microclimate simulation model*. USDA Forest Service, Research paper INT-414, Intermountain Research Station, Ogden.
- Jensen, M.E. and Haise, H.R., 1963. Estimating evapotranspiration from solar radiation. *J. Irrig. Drainage Div. ASCE*, **89**: 15-41.

- Kimball, J. S., S. W. Running, and R. Nemani. 1997. An improved method for estimating surface humidity from daily minimum temperature. *Agricultural and Forest Meteorology* **85**:87-98.
- Kumar, L., Skidmore, A.K. and Knowles, E., 1997. Modelling topographic variation in solar radiation in a GIS environment. *International Journal for Geographical Information Systems*, **11**(5): 475-497.
- Müller, G. 1989. Untersuchungen zur Bestimmung der Verdunstung im voralpinen Raum. *Zür. Geogr. Schr.* **36**: 1-224.
- Prentice, I.C., Cramer, W., Harrison, S.P., Leemans, R., Monserud, R.A. & Solomon A.M. 1992. A global biome model based on plant physiology and dominance, soil properties and climate. *Journal of Biogeography* **19**:117-134.
- Rich, P.M., Hetrick, W.A. and Savings, S.C., 1995. *Modelling topographical influences on solar radiation: manual for the SOLARFLUX model*. LA-12989-M, Los Alamos National Laboratories, Los Alamos.
- Running, S.W. 1994. Testing FOREST-BGC ecosystem process simulations across a climatic gradient in Oregon. *Ecological Applications* **4**(2): 238-247.
- Running, S.W. and Gower, S.T. 1991. FOREST-BGC, A general model of forest ecosystem processes for regional applications: II. Dynamic carbon allocation and nitrogen budgets. *Tree Physiology* **9**: 147-160.
- Running, S. W., R. R. Nemani, and R. D. Hungerford. 1987. Extrapolation of synoptic meteorological data in mountainous terrain and its use for simulating forest evaporation and photosynthesis. *Canadian Journal of Forest Research* **17**:472-483.
- Schrödter, H. 1985. *Verdunstung. Anwendungsorientierte Messverfahren und Bestimmungsmethoden*. Springer Verlag, Berlin.
- Stillman, S. T., J. P. Wilson, C. Daly, M. F. Hutchinson, and P. E. Thornton. 1996. *Comparison of ANUSPLIN, MTCLIM-3D, and PRISM precipitation estimates*. in The Third International Conference/Workshop on Integrating GIS and Environmental Modeling. National Center for Geographic Information and Analysis, Santa Fe, NM.
- Thornton, P.E., 1998. *Regional ecosystem simulation: combining surface- and satellite-based observations to study linkages between energy and mass budgets*. Ph.D. Thesis, University of Montana, Missoula, MT, 200 pp.
- Thornton, P.E., Hasenauer, H. and White, M.A., 2000. Simultaneous estimation of daily solar radiation and humidity from observed temperature and precipitation: an application over complex terrain in Austria. *Agricultural and Forest Meteorology*, **104**(4): 255-271.
- Thornton, P.E. and Running, S.W., 1999. An improved algorithm for estimating incident daily solar radiation from measurements of temperature, humidity, and precipitation. *Agricultural and Forest Meteorology*, **93**(4): 211-228.
- Thornton, P.E., Running, S.W. and White, M.A., 1997. Generating surfaces of daily meteorological variables over large regions of complex terrain. *Journal of Hydrology*, **190**(3-4): 214-251.
- Tuhkanen, S. 1980. Climatic parameters and indices in plant geography. *Acta Phytogeographica Suecica* **67**:1-105.
- Turc, L., 1963. Evaluation des besoins en eau d'irrigation, évapotranspiration potentielle, formulation simplifiée et mise à jour. *Ann. Agron.*, **12**: 13-49.
- Zimmermann, N.E. and Kienast, F., 1999. Predictive mapping of alpine grasslands in Switzerland: species versus community approach. *Journal of Vegetation Science* **10**(4): 469-482.